

## Growth mechanism and the order of appearance of diamond (111) and (100) facets

Biwu Sun, Xiaopin Zhang, and Zhangda Lin

*Laboratory for Surface Physics, Institute of Physics, Academia Sinica, Beijing 100080, People's Republic of China*

(Received 9 July 1992; revised manuscript received 19 October 1992)

Experiments with local gas feeds of methane or acetylene indicate that both  $C_2H_2$  and  $CH_3$  contribute to the growth of (111) surfaces, whereas only  $CH_3$  contributes to that of the (100) surface. High-resolution electron-energy-loss spectroscopy has been used to investigate the termination modes of grown diamond (111) and (100) facets. The diamond (111) facets grown at  $800^\circ C$  and 0.2%  $CH_4$  consist of (111) faces and  $\{110\}$  steps; atomic deuterium first replaces the hydrogen atoms adsorbed on (111) faces, and the growth rate of (111) facets is controlled by the concentration of  $C_2H_2$  at the film surface. After further growth of grown diamond (111) facets at 0.2%  $CH_4$  of local feed for 30 min,  $CH_3$  vibrational modes on (111) facets have been detected. The diamond (100) facets grown at  $800^\circ C$  and 1.0%  $CH_4$  are terminated with  $CH_2$  radicals. Besides the  $CH_2$  vibration loss, CH bend loss of monohydrogenated dimer is detected for the (100) facets grown at  $1000^\circ C$ . Based on the above results, it is suggested that the morphology of diamond film is controlled by the ratio of  $C_2H_2$  to  $CH_3$  concentration at the film surface. The higher the ratio, the faster the (111) facets grow, and thus (100) facets will be shown. Otherwise, (111) facets appear. This explains the rule of diamond crystalline appearance very well.

### I. INTRODUCTION

The mechanism of chemical-vapor-deposited (CVD) diamond film has attracted more and more attention of researchers in recent years, both because further technological advancement requires a detailed understanding of the fundamental phenomena responsible for diamond growth, and the study of diamond growth offers a truly unique opportunity for understanding the chemistry of a CVD process. The Russian school of Derjagin and co-workers<sup>1-3</sup> developed a model for diamond nucleation and growth based on macroscopic concepts of classical nucleation theory and adsorption-deposition kinetics and equilibrium, but their theory did not predict possible growth species or specific reactions taking place at the surface. For several years, the prevalent view for growth in hot filament<sup>4</sup> (HF) and microwave plasma<sup>5</sup> environments has been that the methyl radical is primarily responsible for diamond growth.<sup>6-8</sup> But there has been a dispute about whether it is suitable for the growth of diamond (111) surfaces. The first mechanism describing diamond (111) growth in detail was proposed by Tsuda, Nakajima, and Oikawa,<sup>9,10</sup> but this mechanism involved  $CH_3^+$  cations or a positively charged surface. Later Chu *et al.*<sup>11</sup> proposed that the methyl radical is the dominant growth precursor under HF CVD conditions for all (111), (100), and (110) facets. Martin and co-workers<sup>12,13</sup> showed that methyl or methane is much more effective than acetylene for growing diamond films and acetylene produces lower-quality films than methyl or methane. However, Frenklach and co-workers<sup>14-17</sup> proposed that acetylene, which is present in greater quantities than  $CH_3$  under typical HF CVD conditions,<sup>18-20</sup> is the primary growth precursor on diamond (111).

For the growth of diamond (100) surfaces Harris<sup>21</sup> recently proposed a growth mechanism involving only neutral  $CH_3$  and hydrogen atoms using a nine-carbon model

compound [bicyclononane (BCN)], and the predicted growth rate on (100) surface agreed well with experiment. But the steric repulsion for the H-H site on BCN is different from that on the diamond (100) surface. On the diamond (100) surface terminated by  $CH_2$  radicals, there is only an internuclear H-H spacing of about 0.77 Å, or nearly the same as that in the  $H_2$  molecule, 0.74 Å. As this has to be a nonbonding interaction, very strong steric repulsions between neighboring hydrogen atoms would be expected. Mehandru and Anderson<sup>22</sup> proposed that the strain on the (100) surface is relieved to a certain degree by the H moving apart with the result that the  $CH_2$  angles decrease about  $25^\circ$  from the ideal tetrahedral angle. This will affect the growth of the diamond (100) surface strongly.

Kobashi *et al.*<sup>23</sup> found that the film surface consists of triangular (111) diamond faces for  $CH_4$  concentrations  $c < 0.4\%$ , whereas square (100) faces are predominant above 0.4%  $CH_4$ . Matsumoto, Sato, and Tsutsumi<sup>24</sup> showed that diamond crystals with cubic habit appeared at high substrate temperatures. Other researchers have studied the morphologies of diamond films at different  $O_2$  concentrations, temperatures of substrate and filament, pressures, and filament geometries.<sup>25-32</sup>

According to Hartman's<sup>33</sup> periodic-bond-chain (PBC) theory, which successfully described the morphology of natural diamond (ND), the (100) faces of diamond have the highest growth rate, and should not appear as diamond facets. However, the experimental data observed<sup>23-32</sup> strongly contradict this prediction. The morphology of diamonds synthesized by high-pressure-high-temperature (HPHT) methods<sup>34</sup> shows that cubic habit appears at low temperature, or equivalently, at supersaturation, and it is also not valid for CVD methods because (100) faces appear at high temperatures in the HF CVD device.<sup>24</sup> The key factor of controlling facet appearance is still unknown; this is be-

cause the mechanism of diamond growth is unclear so far.

In this paper, we first investigate the termination modes of diamond (111) and (100) facets deposited at different conditions using high-resolution electron-energy-loss spectroscopy (HREELS) and discuss the growth mechanism of diamond (111) and (100) facets, and then study the rule of diamond crystalline appearance.

## II. EXPERIMENT

The HF CVD design is similar to that of Chu *et al.*<sup>11</sup> and Yarbrough, Tankala, and Debroy.<sup>35</sup> In typical experiments premixed mixtures of  $\text{CH}_4 + \text{H}_2/\text{CH}_4 + \text{O}_2 + \text{H}_2$  were fed to the chamber. This is called remote feed. In the experiments that are used to measure the growth rates of diamond (100) or (111) surfaces, a 3-mm-o.d. stainless-steel tube was put just above the substrate so as to direct gas of  $\text{CH}_4$  or  $\text{C}_2\text{H}_2$  to substrate surface immediately. This is called local feed. This arrangement makes concentrations at film surface rely not solely on diffusion from hot filament, and reduces the extent of gas-phase chemistry. The substrates used were two diamond single crystals, cubic and half octahedral, respectively, about 1.5 mm in size. They were slightly pressed side by side on a platinum ribbon. Scanning electron microscopy (SEM) identified that the surfaces of the single crystals were smooth. Before and after growth, the diamond single crystals were weighed. The growth rates were calculated according to the effective surface areas of single crystals. The effective surface areas did not include the area of the bottom surface attached to the Pt ribbon. The typical experimental parameters were as follows: pressure, 50 torr; filament temperature, 2000°C; substrate temperature, 800°C; gas flux, 100 SCCM (SCCM denotes cubic centimeter per minute at STP); filament to substrate distance ( $D_{fs}$ ), 8 mm; and  $\text{CH}_4$  concentration, 0.6%. Hereafter, if there is no special note, the experimental parameters are those listed above.

HREELS measurements were performed in a Leybold ELS-22, which attained a base vacuum of  $1 \times 10^{-10}$  mbar. When dosing the sample with atomic hydrogen, deuterium, and oxygen at  $1 \times 10^{-6}$  mbar, the  $\text{H}_2$ ,  $\text{D}_2$ , or  $\text{O}_2$  leaked into the 220-mm-i.d. chamber is dissociated by the filament at 2000°C. Temperature measurement was made by a thermocouple (NiCr-NiAl) spot-welded to the Ta side of the support fixture, and the sample was heated to 700°C when dosing. Diamond films were deposited on Si(100) substrates at different conditions, and HREELS was used to analyze the samples.

## III. RESULTS AND DISCUSSION

### A. Growth rates of diamond (100) and (111) facets

Figure 1 shows the growth thickness of diamond (111) and (100) surfaces against deposition time. The growth thickness is directly proportional to the deposition time. The diamond growth rate is defined as a thickness increment per unit time. From Fig. 1, it is known that the growth rates of the (100) surface with 0.8%  $\text{CH}_4$  and

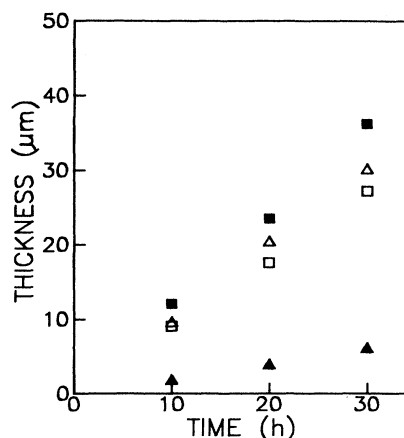


FIG. 1. Diamond film thickness against deposition time. Solid squares, (100) surface with 0.8%  $\text{CH}_4$  local feed; open squares, (111) surface with 0.8%  $\text{CH}_4$  local feed; solid triangles, (100) surface with 0.4%  $\text{C}_2\text{H}_2$  local feed; open triangles, (111) surface with 0.4%  $\text{C}_2\text{H}_2$  local feed.

0.4%  $\text{C}_2\text{H}_2$  are 1.4 and 0.2  $\mu\text{m}/\text{h}$ , respectively, whereas the growth rates of the (111) surface with 0.8%  $\text{CH}_4$  and 0.4%  $\text{C}_2\text{H}_2$  are 0.9 and 1.0  $\mu\text{m}/\text{h}$ , respectively. The growth rate of the (100) surface with 0.8%  $\text{CH}_4$  local feed is much higher than that with 0.4%  $\text{C}_2\text{H}_2$  local feed, whereas the growth rate of the (111) surface with 0.4%  $\text{C}_2\text{H}_2$  local feed is almost the same as that with 0.8%  $\text{CH}_4$  local feed. If the concentration of  $\text{C}_2\text{H}_2$  is equal to that of  $\text{CH}_4$ , it is believed that the growth rate of (111) facets with  $\text{C}_2\text{H}_2$  local feed is higher than that with  $\text{CH}_4$  local feed. In fact, the growth rate of (111) facets with 0.8%  $\text{C}_2\text{H}_2$  local feed reached 1.5  $\mu\text{m}/\text{h}$ . Because there is much amorphous carbon in the film, the measured growth rate is not used to compare with that of (111) facets with 0.8%  $\text{CH}_4$ . It is believed that when one hydrocarbon species is fed locally, the concentrations of other hydrocarbon species at the film surface are very low. So the above results indicate that both  $\text{C}_2\text{H}_2$  and  $\text{CH}_4$  contribute to the growth of the diamond (111) surface, whereas only  $\text{CH}_4$  to the growth of the (100) surface.

### B. Growth mechanism of diamond (111) facets

Figure 2(a) shows diamond film morphology at 0.2%  $\text{CH}_4$  remote feed and 800°C. The film morphology consists of triangular (111) facets. The vibrational loss spectrum for grown diamond (111) facets of this sample is shown in Fig. 3(a). Intense losses occur at 155 and 365 meV, with smaller losses at 110, 310, and 460 meV. Compared with characteristic frequencies of molecular subgroups  $\text{CH}_x$ ,<sup>36</sup> the spectrum is consistent with that of CH radicals. We assign 155-meV loss to CH bend vibration, 365-meV loss to CH stretch, 110-meV to C-C stretch, and 310 and 460 meV to the first and second overtones of CH bend, respectively. The morphologies of diamond films deposited at 0.2%  $\text{CH}_4$  remote feed and 900 and 1000°C, respectively, also demonstrate the tri-

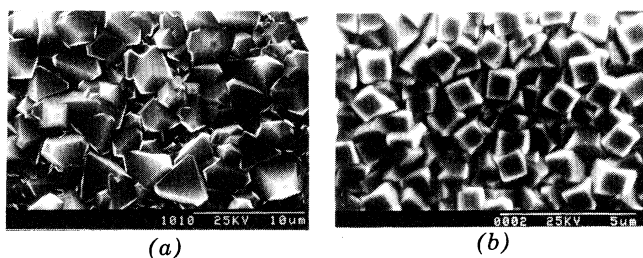


FIG. 2. SEM surface morphology of diamond films deposited at 800°C and (a) 0.2% and (b) 1.0% CH<sub>4</sub> remote feed.

angular facets. The HREELS spectra of these samples are shown in Figs. 3(b) and 3(c). They have loss peaks similar to that grown at 800°C, but with the increase of substrate temperature the loss peaks of CH stretch strengthen.

For the diamond (111) surface terminated by CH radicals, CH stretch vibration moment is normal to the surface and CH bend vibration moment is parallel to the surface. According to the selection rule,<sup>37</sup> the vibrational mode with only parallel moment should be absent. Is the selection rule not valid? When atomic deuterium dosed the grown diamond (111) facets for 10 min, the HREELS spectrum [Fig. 4(a)] shows only strong C-D stretch (270 meV) and C-H bend (155 meV) losses. The loss peaks of C-D bend (112 meV) and C-H stretch (365 meV) are very weak. This indicates that there are two kinds of CH radicals on grown diamond (111) facets: one C-H stretch vibration moment is perpendicular to the (111) facet, and another C-H stretch vibration moment is parallel to the (111) facet. If we suggested that the grown diamond (111) facet consists of (111) faces and {110} face steps, the above experiment results can be explained very well because the C-H bond on the (110) face is approximately parallel to the (111) facet. This suggestion agrees remarkably with Frenklach's mechanism;<sup>14</sup> along its grown path the (111) surface consists of (111) face and {110} steps.

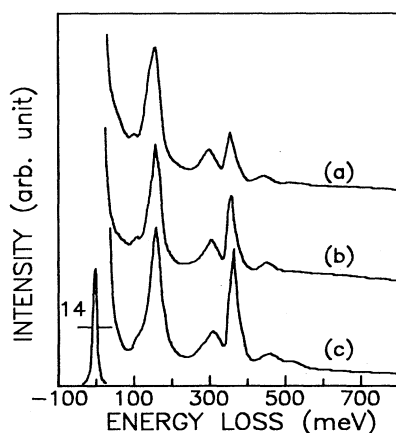


FIG. 3. High-resolution electron-energy-loss spectra of grown diamond (111) facets with 0.2% CH<sub>4</sub> remote feed and at (a) 800°C, (b) 900°C, and (c) 1000°C.

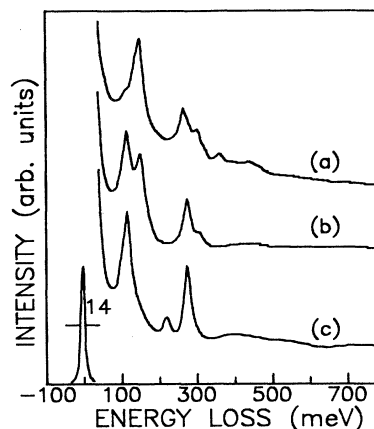


FIG. 4. HREELS of (a) grown diamond (111) facets dosed with atomic deuterium for 10 min, (b) dosed again for another 5 min, and (c) yet again dosed for 10 min.

After atomic deuterium had reacted with (111) facets for another 5 min, an intense loss peak of C-D bend (112 meV) appeared, and the intensity of the C-H bend vibrational loss peak lessened [Fig. 4(b)]. Proceeding again for another 10 min, dosing with atomic deuterium, the C-H bend loss disappeared [Fig. 4(c)]. The above results show that atomic deuterium first reacts with hydrogen atoms adsorbed on {110} steps. According to Frenklach's mechanism,<sup>14</sup> the growth of the (111) surface included the kernel formation and propagation stages. In the kernel formation the first event was the activation of a surface carbon by the H abstraction, and then the C<sub>2</sub>H<sub>2</sub> or CH<sub>3</sub>/CH<sub>4</sub> species was added. But in the propagation stage, the (111) surface was grown along the [01 $\bar{1}$ ] direction with only acetylene, and hydrogen atoms are not consumed but only migrate from a lower to an upper layer. The fact that atomic hydrogen atoms in the gas phase prefer to react with hydrogen adsorbed on the (111) face also supports Frenklach's mechanism. The growth of the diamond (111) surface along the [01 $\bar{1}$ ] direction with C<sub>2</sub>H<sub>2</sub> species avoids steric repulsion and reduces surface energy because the (111) surface is always terminated by CH radicals during the growth.

From Fig. 3(a) it is known that both the losses of C-H bend on {110} steps and C-H stretch on (111) faces are strong. The more the kernels grow, the more the steps form, and the stronger the loss peak of C-H bend vibration becomes. The faster the propagation process, the fewer the steps, and relatively the larger the intensity of loss peak of C-H stretch on (111) faces. So the rate of the formation of kernel is on the same order of magnitude with that of the propagation stage. Frenklach and Wang<sup>16</sup> argued that the reaction "bottleneck" of diamond (111) facet growth is the formation of active sites. However, from Fig. 3(a) the intensity of C-H bend of {110} steps is twice that of C-H stretch on (111) faces. This means that there are many steps on the grown diamond (111) facets, and the initiation process, the formation of active sites, is not the reaction bottleneck. Since

acetylene addition is assumed to proceed without activation energy,<sup>15</sup> it turns out that the growth rate of diamond (111) facets is controlled by the concentration of  $C_2H_2$  at film surface. Of course the  $C_2H_2$  concentration should not be too high because  $C_2H_2$  easily forms nondiamond carbon.<sup>38</sup>

From the above discussion, it is explained very well that with the increase of substrate temperature the loss peak of CH stretch strengthens. When the substrate temperature increases, the concentration of  $C_2H_2$  at the film surface increases, and that of  $CH_4$  decreases.<sup>39</sup> So with the increase of the substrate temperature, the amount of steps decrease, the rate of the propagation process increases, and consequently the loss peak of CH stretch strengthens. It should be noted that when (111) facets appear, the concentration of  $C_2H_2$  at film surface is lower than that of  $CH_4$ . (This will be discussed in detail in Sec. III D.) This is possibly the reason that the growth rate of the (111) surface is controlled by  $C_2H_2$  concentration at the film surface.

Waclawski *et al.*<sup>40</sup> measured the vibrational modes of hydrocarbon on polished natural diamond (111) surfaces using HREELS and found the ND (111) surface is terminated by  $CH_3$  radicals [Fig. 5(a)]. If all carbon sites on the (111) surface are covered by  $CH_3$ , this should cause strong steric repulsion and hence shift the frequencies of  $CH_3$  vibration. However, there was no detectable shift of  $CH_3$  loss peaks observed compared with the  $CH_3$  subgroup.<sup>36</sup> It seems that the absence of a detectable shift is due to the existence of high density of defect on the (111) surface by polishing. Defect "dilutes" the population of  $CH_3$  on the surface. The grown diamond film with (111) facets was deposited again for 30 min at 0.2%  $CH_4$  local feed and 800°C substrate temperature. SEM showed no change of film morphology. HREELS spectrum is shown in Fig. 5(b). Compared with the characteristic frequencies of molecular subgroup  $CH_3$ ,<sup>36</sup> the three loss peaks near 160 meV are identical to those of  $CH_3$  *s* deformation (167 meV),  $CH_3$  *d* deformation (179 meV), and  $CH_3$  rock

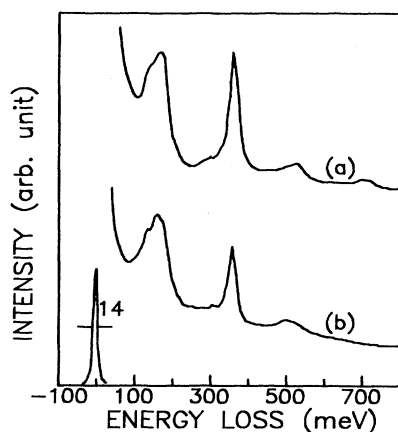


FIG. 5. High-resolution electron-energy-loss spectra of (a) ND (111) (Ref. 40), (b) sample of Fig. 3(a) grown proceedingly with 0.2%  $CH_4$  local feed for 30 min.

vibration (127 meV). This means that the (111) facets deposited with 0.2%  $CH_4$  local feed are terminated by  $CH_3$  radicals. The reason that the (111) facets grown with 0.2%  $CH_4$  local feed differ from that with 0.2%  $CH_4$  remote feed is possibly that in the experiment of 0.2%  $CH_4$  local feed only  $CH_3/CH_4$  species are the primary precursor, but in that of 0.2%  $CH_4$  remote feed, the concentrations of  $CH_4$  and  $C_2H_2$  are almost the same.<sup>41</sup> For the growth of diamond (111) surfaces with  $CH_3$  radicals, Harris, Belton, and Blint<sup>38</sup> proposed a simple H-abstraction/ $CH_3$ -addition mechanism. According to this mechanism, there are enough  $CH_3$  radicals on grown diamond (111) surface. Frenklach and Spear<sup>14</sup> also proposed that  $CH_3/CH_4$  form kernels on (111) surfaces. So we propose that when only  $CH_3/CH_4$  contributes to the growth of diamond (111) facets, the (111) facets are terminated by  $CH_3$  radicals. From Sec. III A, it is known that  $CH_4/CH_3$  indeed contributes to the growth of the (111) surface. But if all carbon sites on the (111) surface are covered by  $CH_3$ , this should cause a strong steric repulsion and hence would shift the frequencies of  $CH_3$  vibration. However, there was no detectable shift of  $CH_3$  loss peaks observed compared with the  $CH_3$  subgroup.<sup>36</sup> Due to the strong steric repulsion between neighboring  $CH_3$  radicals on the (111) surface, the formation of one  $CH_3$  kernel adjacent to another  $CH_3$  is difficult, and the  $CH_3/CH_4$  species in the gas phase prefer to form kernels at nearest-neighbor sites of present kernels. So we suggest that the diamond (111) facets deposited at 0.2%  $CH_4$  local feed consist of nearest-neighbor  $CH_3$  kernels, for the (111) surface rough on atomic scale avoids the steric repulsion during the growth of the (111) surface with  $CH_3/CH_4$  species. This kind of surface is similar to the polished ND surface in some case. From our experiment it is uncertain whether  $C_2H_2$  species contribute to the formation of kernels.

### C. Grown diamond (100) surface

The morphology of diamond film deposited at 1.0%  $CH_4$  of remote feed and 800°C consisted of square (100) facets [Fig. 2(b)]. The vibrational loss spectrum for diamond (100) facets grown at 800°C is shown in Fig. 6(a). Intense losses occur at 156, 180, and 372 meV, with three smaller losses at 110, 310, and 530 meV. Compared with the characteristic frequencies of molecular subgroups  $CH_x$ ,<sup>36</sup> the spectrum is consistent with that of the  $CH_2$  radical, which has its scissor vibration at 179 meV, wag at 157 meV, twist at 150 meV, rock at 108 meV, and stretch at 370 meV. We assign 372-meV loss to  $CH_2$  stretch, 110 meV to  $CH_2$  rock, 180 meV to scissor, and 156 meV to the overlapping of wag and twist. The loss at 310 meV is the overtone of the loss at 156 meV, and the loss at 530 meV is the combination of  $CH_2$  wag and stretch. But it is very interesting to note that there is no detectable shift of the losses of  $CH_2$  on the diamond (100) surface compared with  $CH_2$  subgroups.

The HREELS spectrum of the diamond film deposited at 1000°C is shown in Fig. 6(b). The spectrum is similar to that of the diamond film deposited at 800°C, and there

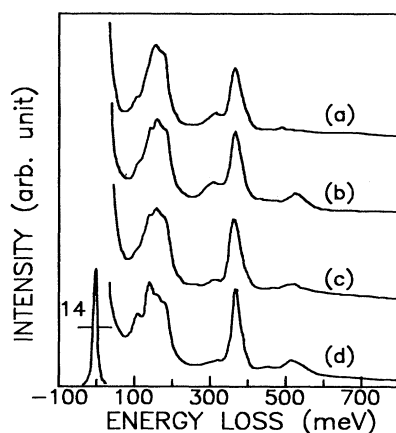
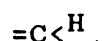


FIG. 6. High-resolution electron-energy-loss spectra of (a) diamond (100) facets grown at 800 °C and 1.0% CH<sub>4</sub>, (b) (100) facets grown at 1000 °C, (c) the sample of (a) dosed with atomic hydrogen, and (d) dosed with oxygen.

is also no detectable shift about CH<sub>2</sub> vibrations, but a medium loss appears at 140 meV. For diamond (100) surface, Hamza, Kubiak, and Stulen<sup>42</sup> found a 1×1 low-energy electron-diffraction (LEED) pattern on warming from 500 to 750 K which was assigned to the dihydrogenated surface. On heating to over 1300 K, hydrogen desorbed and a 2×1 surface structure developed which was believed to be due to a monohydrogenated surface with elongated surface C-C dimer bonds.<sup>22</sup> Tsuno *et al.*<sup>43</sup> and Sutcu<sup>44</sup> recently observed grown diamond surfaces on atomic level resolution by scanning-tunneling microscopy (STM) and atomic-force microscopy (AFM), respectively, and found a (2×1) reconstruction on the (100) surface grown at 1000 °C. According to Mehandru's structure model,<sup>22</sup> the C-H bond of the monohydrogenated dimer is similar to that of



and its C-H bend loss should shift down relative to the *sp*<sup>3</sup>-hybridized C-H bend but should be higher than that of



The bend vibration of the C-H bond of the monohydrogenated dimer has moment normal to the surface. According to the selection rule,<sup>37</sup> its loss peak will be present. Shimanouchi's results<sup>36</sup> indicated that the frequency of



bend vibration is at about 129 meV. So we assign the loss at 140 meV to the C-H bend vibration of the monohydrogenated dimer. From Fig. 6(b), it is known that the C-H bend loss of the dimer is lower than that of the CH<sub>2</sub> wag; the amounts of dimers should be similar to that of CH<sub>2</sub> radicals. Also, no detectable shift of CH<sub>2</sub> vibration was observed. If the monohydrogenated dimers are not separated uniformly, there must be at least several CH<sub>2</sub>

radicals at adjacent sites. In this case, the repulsion among neighboring hydrogen atoms still exists, and there should be detectable a shift of CH<sub>2</sub> losses. So it turns out the monohydrogenated dimers should be dispersed uniformly.

When the surface of diamond film grown at 800 °C was dosed with atomic hydrogen for 10 min [Fig. 6(c)], the loss peak at 140 meV also appeared and the losses of CH<sub>2</sub> scissor, wag, and twist lessened. But further dosing with atomic hydrogen did not produce the further change of the loss peaks. If only one hydrogen is abstracted among CH<sub>2</sub> radicals, there is only one vacant site and reconstruction should not be expected. If more hydrogen atoms are abstracted, adjacent vacant sites would dimerize.<sup>22</sup> During the process of diamond growth, the hydrogen atoms in gas phase abstract the adsorbed hydrogen.<sup>16</sup> Growth at higher temperature and dosing only with atomic hydrogen both cause more adsorbed hydrogen to be abstracted. Because the situation of separated C-H radicals is between that of the dihydrogenated (100) surface and the monohydrogenated dimer, it is suggested that there are many separately *sp*<sup>2</sup>-hybridized C-H radicals each with one vacant site on the diamond (100) facets grown at 800 °C. Its C-H bond is normal to the surface and its C-H bend has no normal moment. According to the selection rule,<sup>37</sup> the loss peak of the C-H bend does not appear. It is consistent with the experimental result. From Fig. 6(a) it is known that there is no detectable shift of CH<sub>2</sub> loss and the loss of the bend of the monohydrogenated dimer is not observed. So it is suggested that *sp*<sup>2</sup>-hybridized C-H radicals on grown diamond (100) surfaces are in enough quantity and are uniformly dispersed. The uniformly dispersed C-H radicals relax greatly the repulsion between the neighbor hydrogen atoms on the (100) surface. After the growth, the sample was exposed to the atmosphere and then measured by HREELS. In general, the *sp*<sup>2</sup>-hybridized C-H radicals are active. But the above results show that the CH<sub>2</sub>-terminated (100) surface with uniformly separated CH radicals is relatively stable. This kind of structure avoids the strong steric repulsion on the (100) surface between adjacent hydrogen atoms and the vacant sites will offer the active site for the next addition of suitable hydrocarbon species.

When the (100) facets grown at 800 °C were dosed with oxygen for 10 min, the spectrum [Fig. 6(d)] shows that the losses of CH<sub>2</sub> wag and scissor lessen clearly, the loss of C-H bend of monohydrogenated dimer strengthens, and an intensive loss at 110 meV appears. Oxygen causes more adsorbed hydrogen atoms on (100) surface to be abstracted. Compared with the characteristic frequency of C-C stretch,<sup>36</sup> the loss peak at 110 meV is assigned to the C-C stretch. The role of oxygen causing more hydrogen to be abstracted will speed the diamond growth.

#### D. Principal factor controlling morphology of diamond film surface

The morphologies of diamond films deposited at different CH<sub>4</sub> concentrations are identical to those of Kobashi *et al.*,<sup>23</sup> i.e., the film surface consists of (111) facets for CH<sub>4</sub> concentration *c* < 0.4%, whereas (100)

facets are predominant above 0.4%  $\text{CH}_4$ . With 0.2% and 0.4% oxygen addition at 3.0%  $\text{CH}_4$  [Figs. 7(a) and 7(b)], (100) facets are predominant. At 0.6%  $\text{O}_2$ , the film shows crystal with both (111) and (100) facets [Fig. 7(c)]. At 0.8%  $\text{O}_2$ , the film is made up of (111) facets only [Fig. 7(d)]. Baik and Eun<sup>27</sup> obtained similar results. The change of distance between filament and substrate also alters the morphology of diamond films. SEM shows that at  $D_{fs}=7$  and 10 mm with 0.6%  $\text{CH}_4$ , the (100) facets dominate the surfaces of diamond films [Figs. 8(a) and 8(b)]. When  $D_{fs}=14$  mm, the film surface consists of both (100) and (111) facets [Fig. 8(c)]. At  $D_{fs}=18$ , triangular (111) facets are the predominant surface morphology [Fig. 8(d)].

Harris and Weiner<sup>41</sup> measured the gas-phase composition at the surface of a growing diamond film as a function of the initial  $\text{CH}_4$  fraction and, for a 2%  $\text{CH}_4$  fraction, as a function of added oxygen [Fig. 9]. From Fig. 9(a) it is known that the concentrations of  $\text{C}_2\text{H}_2$  and  $\text{CH}_4$  both increase with the initial  $\text{CH}_4$  fraction. When the initial  $\text{CH}_4$  fraction is larger than 0.5%, the concentration of  $\text{C}_2\text{H}_2$  at the film surface is higher than that of  $\text{CH}_4$ . From the tendency of concentration change, it can be rationally proposed that the concentration of  $\text{CH}_4$  is higher than that of  $\text{C}_2\text{H}_2$  when initial the  $\text{CH}_4$  fraction is lower than 0.5%. Hsu's results<sup>45</sup> verified this tendency. When the fraction of added  $\text{O}_2$  is lower than 0.8%, the concentration of  $\text{C}_2\text{H}_2$  at the film surface is higher than that of  $\text{CH}_4$  [Fig. 9(b)]. It can also be expected rationally that the concentration of  $\text{CH}_4$  is higher than that of  $\text{C}_2\text{H}_2$  when fraction of added  $\text{O}_2$  is larger than 0.8%. Harris *et al.*<sup>46</sup> also measured the concentrations of  $\text{CH}_4$ ,  $\text{C}_2\text{H}_2$ , and other species at the substrate surface at different  $D_{fs}$  (Fig. 10). When the distance was less than 15 mm, the concentration of  $\text{CH}_4$  at substrate surface was lower than that of  $\text{C}_2\text{H}_2$ ; otherwise the concentration of  $\text{CH}_4$  was higher than that of  $\text{C}_2\text{H}_2$ . We found that there is a re-

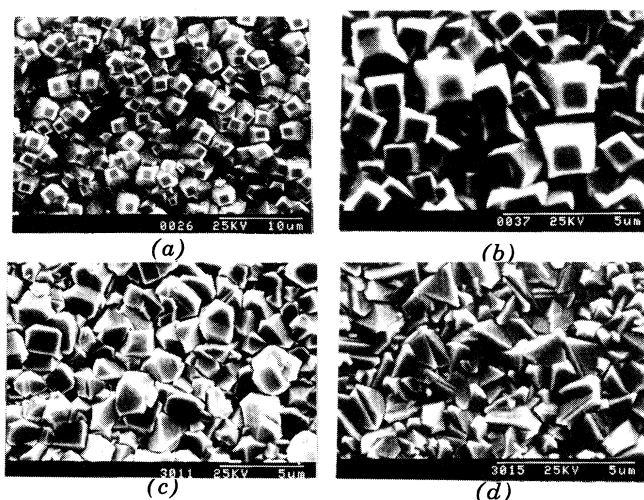


FIG. 7. SEM morphology of diamond films deposited at 3%  $\text{CH}_4$  and (a) 0.2%, (b) 0.4%, (c) 0.6%, and (d) 0.8%  $\text{O}_2$ .

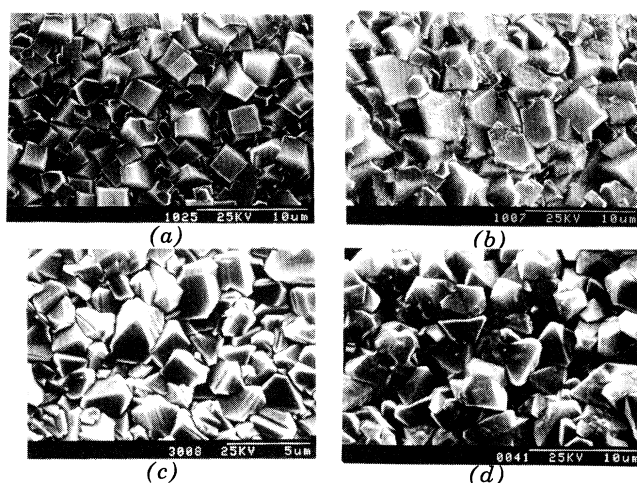


FIG. 8. SEM morphology of diamond films deposited at 0.6%  $\text{CH}_4$  and 800°C. Distances between filament and substrate are (a) 7 mm, (b) 10 mm, (c) 14 mm, and (d) 18 mm.

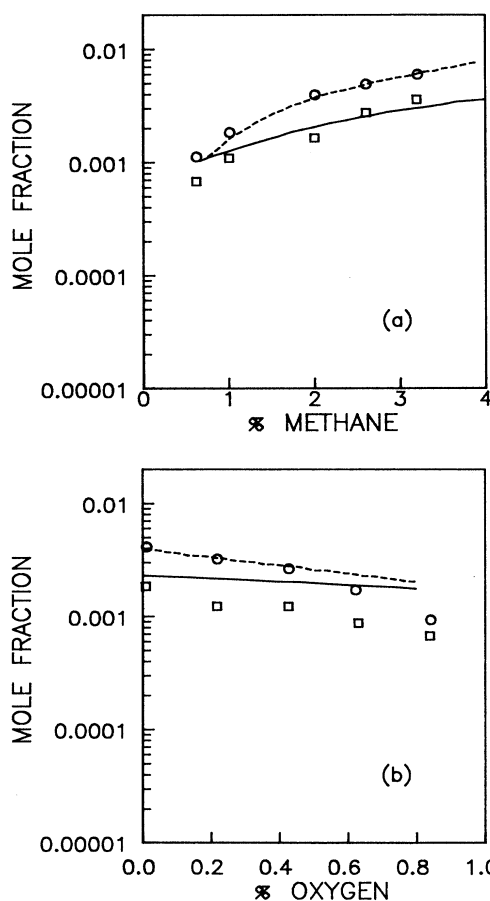


FIG. 9. Comparison between measured and calculated species mole fractions as a function of (a) initial  $\text{CH}_4$  percentage, (b) initial  $\text{O}_2$  percentage for an initial 2%  $\text{CH}_4$  mixture.  $\text{C}_2\text{H}_2$ : open circles (experiment) and dashed line (model);  $\text{CH}_4$ : open squares and dashed line (Ref. 41).

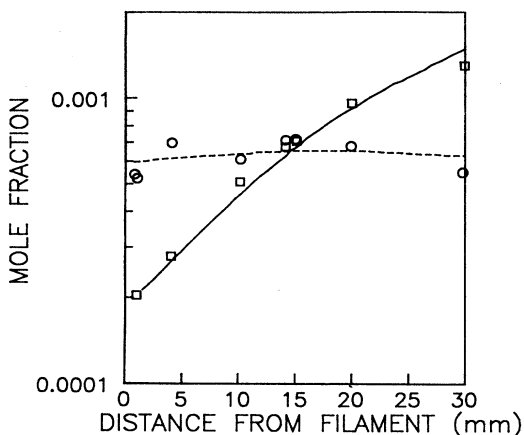


FIG. 10. Mole fractions at the platinum foil as a function of distance from the substrate/probe to the filament. Open circles, C<sub>2</sub>H<sub>2</sub>; open squares, CH<sub>4</sub> (Ref. 46).

markable coincidence between the morphologies of diamond films and the ratio of C<sub>2</sub>H<sub>2</sub> to CH<sub>4</sub> concentration at the substrate surface measured by Harris and co-workers.<sup>41,46</sup> When the concentration of C<sub>2</sub>H<sub>2</sub> at the film surface is higher than that of CH<sub>4</sub>, (100) facets dominate the diamond film surface; otherwise (111) facets appear. Matsumoto, Sato, and Tsutsumi<sup>24</sup> showed that diamond crystals with (100) facets appeared at high substrate temperatures. This fact just matches the results that the concentration of C<sub>2</sub>H<sub>2</sub> increases with substrate temperature, and that of CH<sub>4</sub> decreases with the substrate temperature.<sup>39</sup>

The faces that have the slowest growth rate in the direction of their normal determine the crystal morphology. In fact the crystal morphology is determined by the symmetry of crystal structure, applied force between structure units, defects of crystal lattice, and environmental phase. Considering the effect of crystal structure on the crystalline, Hartman<sup>33</sup> proposed a PBC theory. In his theory, an uninterrupted chain of C-C bonds in diamond is called a PBC, and (111), (110), and (100) faces correspond to *F* (flat), *S* (step), and *K* (kinked) faces, respectively. The *K* face (100) has no PBC, and is predicted to have the highest growth rate, so the (100) faces should not appear as diamond facets, and the facets, even if they appeared, should be rough because they are *K* facets. This theory described successfully the morphology of ND. In HPHT conditions it was found that the growth rates were related to the environmental phase. At low supersaturation of carbon, diamond crystals with cubic habit appeared.<sup>34</sup> In the conditions of HPHT and the formation of natural diamond, diamond is stable thermodynamically.

But in the CVD conditions in which diamond films are deposited, diamond is metastable thermodynamically. This condition determines the dangling bond on the diamond surface is energetically unfavorable. When hydro-

gen adsorbed on a diamond surface, the surface exhibited a 1×1 LEED pattern,<sup>47</sup> and surface carbon atoms maintained sp<sup>3</sup> hybridization.<sup>40</sup> If the lattice is not terminated by hydrogen atoms, the surface will be reconstructed. Pandey<sup>48</sup> proposed a π-bonded chain model for the reconstructed diamond (111)-(2×1) surface, where the dangling bonds form zigzag π-chains. Cluster calculations<sup>49</sup> indicate that the π bond is a possible structure for (100)-(2×1) reconstruction. The reconstructed surface with π bonds is not suitable for diamond growth.<sup>50</sup> During diamond growth in the metastable conditions, the diamond surface must be covered by hydrogen atoms. But this brings about another problem. For a (100) surface terminated by CH<sub>2</sub> radicals, there is very strong steric repulsion between neighboring hydrogen atoms. The diamond (111) surface can be terminated by monolayer CH<sub>3</sub> or monolayer CH radicals. Strong steric repulsions also exist for CH<sub>3</sub> radical coverage. If the diamond (111) surface is covered by CH radicals, it is sure that the (111) surface will be terminated by CH<sub>3</sub> radicals after one monolayer growth along the [111] direction and steric repulsion cannot be avoided. The steric repulsions between adjacent hydrogen atoms cause surface strain and make the surface energy increase. These will strongly affect the growth paths and slow down the growth rates of diamond (100) and (111) surfaces.

Because the (110) surface is a *S* (stepped) face and has no repulsion between adjacent hydrogen atoms, the (110) surface should have the highest growth rate, and does not appear as diamond facets. In fact, the growth rate of the (110) surface with the CVD method is the highest among low-index surfaces,<sup>11</sup> and either methyl-radical- or acetylene-species-based mechanisms can be postulated.<sup>35</sup>

From Sec. III B, it is known that if the mixture of C<sub>2</sub>H<sub>2</sub> and CH<sub>4</sub> is fed, the grown (111) facet is consisted of (111) faces and {110} steps, C<sub>2</sub>H<sub>2</sub> species contribute to the growth along the [011] direction and CH<sub>3</sub>/CH<sub>4</sub> to the formation of kernels, and the growth rate of (111) facets is controlled by the concentration of C<sub>2</sub>H<sub>2</sub> at the film surface, rather than by the creation of active sites. If only CH<sub>4</sub>/CH<sub>3</sub> contributes to the growth of (111) facets, the grown facets are made up of uniformly dispersed CH<sub>3</sub> kernels. From Sec. III C, it is known that grown (100) facets consist of CH<sub>2</sub> radicals and uniformly dispersed sp<sup>2</sup>-hybridized CH radicals and monohydrogenated dimers.

From Sec. III A, it is known that if only CH<sub>4</sub>/CH<sub>3</sub> are primary precursors, the growth rate of the (111) surface is lower than that of the (100) surface. Acetylene does not contribute to the growth of the (100) surface. If the mixture of C<sub>2</sub>H<sub>2</sub> and CH<sub>4</sub>/CH<sub>3</sub> are primary precursors, the growth rate of the (111) surface will rise relative to that of the (100) surface. Because the growth rate of the (111) surface is controlled by the concentration of C<sub>2</sub>H<sub>2</sub> at the film surface, and CH<sub>3</sub> contributes to the growth of (100) facets,<sup>21</sup> the higher the concentration of CH<sub>3</sub> at the film surface, the higher the growth rate of (100) facets, whereas the higher the concentration of C<sub>2</sub>H<sub>2</sub>, the higher the growth rate of (111) facets. Because the CH<sub>3</sub> radical is mainly created by the reaction of

$\text{CH}_4 + \text{H} = \text{CH}_3 + \text{H}_2$ ,<sup>16</sup> the concentration of  $\text{CH}_3$  is proportional to that of  $\text{CH}_4$ . From the above experimental results it is known that the morphology of diamond films is related to the ratio of  $\text{C}_2\text{H}_2$  to  $\text{CH}_4$  at the film surface. So it is suggested that which facets appear between the (100) and (111) facets is determined by the ratio of  $\text{C}_2\text{H}_2$  to  $\text{CH}_3$  concentration at the film surface. When the ratio is higher than a certain value, (111) facets grow faster than (100) facets, and thus (100) facets appear. Otherwise (111) facets appear. There are two steps which determine the morphology of diamond films. First, the different facets of one grain grow competitively, which is controlled by the ratio of  $\text{C}_2\text{H}_2$  to  $\text{CH}_3$  concentration. Second, when the adjacent grains are crowded, the competitive growth between grains begins. The grains whose appeared facets are nearly parallel to the film surface have enough space to grow, and take over those with less favorable orientations. So the appeared facets are approximately parallel to the film surface. This prediction is consistent with the above experimental data.

#### IV. CONCLUSION

For diamond (111) surfaces, it is suggested that both  $\text{C}_2\text{H}_2$  and  $\text{CH}_3/\text{CH}_4$  contribute to the growth of diamond (111) surfaces,  $\text{C}_2\text{H}_2$  to the growth along the  $[01\bar{1}]$  direction, and  $\text{CH}_3/\text{CH}_4$  to the formation of kernels. The growth of diamond (111) surfaces is controlled by the concentration of  $\text{C}_2\text{H}_2$  at the film surface. The diamond (100) surface grown at 800°C consists of  $\text{CH}_2$  radicals and uniformly dispersed  $sp^2$ -hybridized CH radicals, whereas the diamond surface grown at 1000°C is made up of  $\text{CH}_2$  radicals, separated CH radicals, and locally monohydrogenated dimers. These structures are stable and avoid the steric repulsion between neighboring hydrogen atoms on the (100) surface. It is suggested that which facets of diamond crystal appear is determined by the ratio of  $\text{C}_2\text{H}_2$  to  $\text{CH}_3$  concentration at the film surface. When the ratio is higher than a certain value, (111) facets grow faster than (100) facets, and thus (100) facets appear. Otherwise (111) facets appear.

- <sup>1</sup>B. V. Derjagin and D. V. Fedoseev, *Sci. Am.* **233**, 102 (1975).
- <sup>2</sup>B. V. Derjagin and D. V. Fedoseev, *Growth of Diamond and Graphite from the Gas Phase* (Nauka, Moscow, 1977), in Russian [English translation in *Surf. Coat. Technol.* **38**, 131 (1989)].
- <sup>3</sup>D. V. Fedoseev, V. P. Varnin, and B. V. Derjagin, *Russ. Chem. Rev.* **53**, 435 (1984).
- <sup>4</sup>S. Matsumoto, Y. Sato, M. Kamo, and N. Setaka, *Jpn. J. Appl. Phys.* **21**, L183 (1982).
- <sup>5</sup>M. Kamo, Y. Sato, S. Matsumoto, and N. Setaka, *J. Cryst. Growth* **62**, 642 (1983).
- <sup>6</sup>W. G. Eversole, U.S. Patent No. 3030188 (1962).
- <sup>7</sup>R. Mania, L. Stobieski, and R. Pampuch, *Cryst. Res. Technol.* **16**, 785 (1981).
- <sup>8</sup>Y. Hirose and Y. Terasawa, *Jpn. J. Appl. Phys.* **25**, L519 (1986).
- <sup>9</sup>M. Tsuda, M. Nakajima, and S. Oikawa, *J. Am. Chem. Soc.* **108**, 5780 (1986).
- <sup>10</sup>M. Tsuda, M. Nakajima, and S. Oikawa, *Jpn. J. Appl. Phys.* **26**, L527 (1987).
- <sup>11</sup>C. J. Chu, M. P. D'Evelyn, R. H. Hauge, and J. L. Margrave, *J. Appl. Phys.* **70**, 1695 (1991).
- <sup>12</sup>L. R. Martin and M. W. Hill, *J. Mater. Sci. Lett.* **9**, 621 (1990).
- <sup>13</sup>S. J. Harris and L. R. Martin, *J. Mater. Res.* **5**, 2313 (1990).
- <sup>14</sup>M. Frenklach and K. E. Spear, *J. Mater. Res.* **3**, 133 (1988).
- <sup>15</sup>D. Huang, M. Frenklach, and M. Maroncelli, *J. Phys. Chem.* **92**, 6379 (1988).
- <sup>16</sup>M. Frenklach and H. Wang, *Phys. Rev. B* **43**, 1520 (1991).
- <sup>17</sup>D. Huang and M. Frenklach, *J. Phys. Chem.* **95**, 3692 (1991).
- <sup>18</sup>F. G. Celii and J. E. Butler, *Appl. Phys. Lett.* **54**, 1031 (1989).
- <sup>19</sup>M. Frenklach, *J. Appl. Phys.* **65**, 5142 (1989).
- <sup>20</sup>D. G. Goodwin and G. G. Gavillet, *J. Appl. Phys.* **68**, 6393 (1990).
- <sup>21</sup>S. J. Harris, *Appl. Phys. Lett.* **56**, 2298 (1990).
- <sup>22</sup>S. P. Mehandru and A. B. Anderson, *Surf. Sci.* **248**, 369 (1991).
- <sup>23</sup>Koji Kobashi, Kozo Nishimura, Yoshio Kawate, and Takefumi Horiuchi, *Phys. Rev. B* **38**, 4067 (1988).
- <sup>24</sup>S. Matsumoto, Y. Sato, and M. Tsutsumi, *J. Mater. Sci.* **17**, 3106 (1982).
- <sup>25</sup>B. R. Stoner and J. T. Glass, *Appl. Phys. Lett.* **60**, 698 (1992).
- <sup>26</sup>J. F. DeNatale, A. B. Harker, and J. F. Flintoff, *J. Appl. Phys.* **69**, 6456 (1991).
- <sup>27</sup>Young-Joon Baik and Kwang Yong Eun, *Applications of Diamond Films and Related Materials* (Elsevier, New York, 1991), p. 521.
- <sup>28</sup>E. N. Farabaugh, A. Feldman, and L. Robins, in *New Diamond Science and Technology*, Proceedings of the Second International Conference, Washington, DC, 1990, edited by R. Messier, J. T. Glass, J. E. Butler, and R. Roy (Materials Research Society, Pittsburgh, 1991), p. 449.
- <sup>29</sup>R. E. Clausing, L. Heatherly, E. D. Specht, and K. L. More, in *New Diamond Science and Technology* (Ref. 28), p. 575.
- <sup>30</sup>T. Srivinyunon, R. Phillips, C. Cutshow, A. J. Joseph, and Y. Tzeng, in *New Diamond Science and Technology* (Ref. 28), p. 581.
- <sup>31</sup>W. S. Lee, Y. J. Baik, and K. Y. Eun, in *New Diamond Science and Technology* (Ref. 28), p. 593.
- <sup>32</sup>N. Kikuchi, Y. Ohsawa, Y. Tamou, H. Eto, and H. Yamashita, in *New Diamond Science and Technology* (Ref. 28), p. 567.
- <sup>33</sup>P. Hartman, in *Crystal Growth: An Introduction*, edited by P. Hartman (North-Holland, Amsterdam, 1973), p. 367.
- <sup>34</sup>I. Sunagawa, *Jpn. Assoc. Miner. Pet. Econ. Geol.* **3**, 129 (1982).
- <sup>35</sup>W. A. Yarbrough, K. Tankala, and T. Debroy, in *New Diamond Science and Technology* (Ref. 28), p. 341.
- <sup>36</sup>T. Shimanouchi, *Tables of Vibrational Frequencies*, Natl. Bur. Stand. Ref. Data Ser., Natl. Bur. Stand. (U.S.) Circ. No. 39 (U.S. GPO, Washington, DC, 1968), Consolidated Vols. I and II; *J. Phys. Chem. Ref. Data* **6**, 993 (1977).
- <sup>37</sup>H. Ibach and D. L. Mills, *Electron Energy Loss Spectroscopy and Surface Vibrations* (Academic, New York, 1982).
- <sup>38</sup>S. J. Harris, D. N. Belton, and R. J. Blint, *J. Appl. Phys.* **70**, 2654 (1991).
- <sup>39</sup>S. O. Hay, W. C. Roman, and M. B. Colket, *J. Mater. Res.* **5**, 2387 (1990).
- <sup>40</sup>B. J. Waclawski, D. T. Pierce, N. Swanson, and R. J. Celotta, *J. Vac. Sci. Technol.* **21**, 368 (1982).
- <sup>41</sup>S. J. Harris and A. M. Weiner, *J. Appl. Phys.* **67**, 6520 (1990).
- <sup>42</sup>A. V. Hamza, G. D. Kubiak, and R. H. Stulen, *Surf. Sci.* **237**,

- 35 (1990).
- <sup>43</sup>T. Tsuno, T. Imai, Y. Nishibayashi, K. Hamada, and N. Fujimori, *Jpn. J. Appl. Phys.* **30**, 1063 (1991).
- <sup>44</sup>L. F. Sutcu, *Appl. Phys. Lett.* **60**, 1685 (1992).
- <sup>45</sup>W. L. Hsu, *Appl. Phys. Lett.* **59**, 1427 (1991).
- <sup>46</sup>S. J. Harris, D. N. Betton, A. M. Weiner, and S. J. Schmeig, *J. Appl. Phys.* **66**, 5353 (1989).
- <sup>47</sup>B. B. Pate, *Surf. Sci.* **165**, 83 (1986).
- <sup>48</sup>K. C. Pandey, *Phys. Rev. B* **25**, 4338 (1982).
- <sup>49</sup>W. S. Verwoerd, *Surf. Sci.* **103**, 404 (1981); **108**, 153 (1981).
- <sup>50</sup>B. W. Sun, Q. Z. Zhang, S. X. Qi, K. Xie, and Z. D. Lin, *Vac. Sci. Technol.* **11**, 394 (1991) (in Chinese).

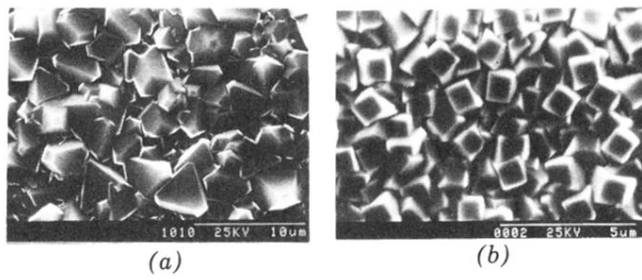


FIG. 2. SEM surface morphology of diamond films deposited at 800°C and (a) 0.2% and (b) 1.0% CH<sub>4</sub> remote feed.

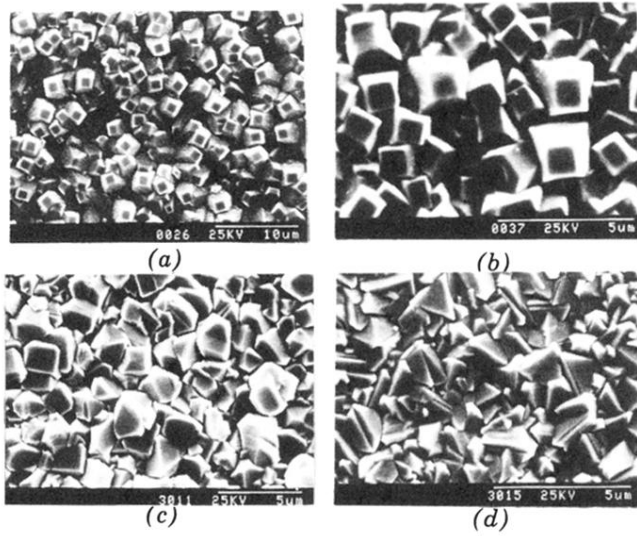


FIG. 7. SEM morphology of diamond films deposited at 3%  $\text{CH}_4$  and (a) 0.2%, (b) 0.4%, (c) 0.6%, and (d) 0.8%  $\text{O}_2$ .

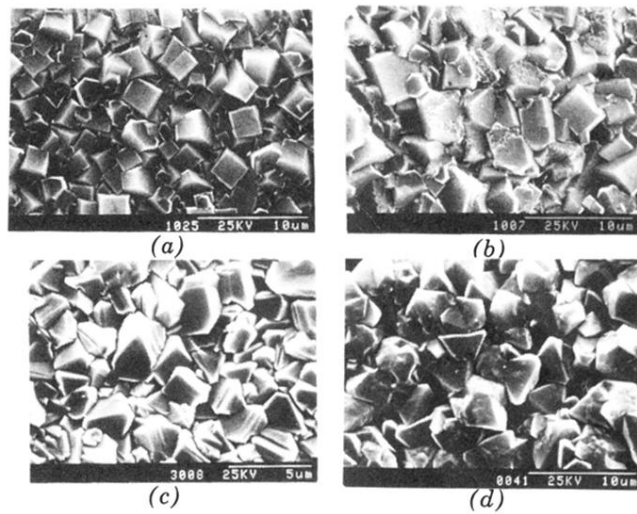


FIG. 8. SEM morphology of diamond films deposited at 0.6% CH<sub>4</sub> and 800°C. Distances between filament and substrate are (a) 7 mm, (b) 10 mm, (c) 14 mm, and (d) 18 mm.